Koitto, Teemu; Kauranne, Heikki; Calonius, Olof; Minav, Tatiana; Pietola, Matti

Experimental Investigation of a Directly Driven Hydraulic Unit in an Industrial Application

Published in:
Proceedings of the 11th International Fluid Power Conference, March 19-21, 2018, Aachen, Germany

DOI:
10.18154/RWTH-2018-224644

Published: 01/01/2018

Document Version
Publisher's PDF, also known as Version of record

Please cite the original version:
Koitto, T., Kauranne, H., Calonius, O., Minav, T., & Pietola, M. (2018). Experimental Investigation of a Directly Driven Hydraulic Unit in an Industrial Application. In H. Murrenhoff (Ed.), *Proceedings of the 11th International Fluid Power Conference, March 19-21, 2018, Aachen, Germany* (Vol. 2). Article 5998 RWTH Aachen University. https://doi.org/10.18154/RWTH-2018-224644

Experimental Investigation of a Directly Driven Hydraulic Unit in an Industrial Application

REVIEWED

Teemu Koitto*, Heikki Kauranne*, Olof Calonius*, Tatiana Minav*, and Matti Pietola*

Aalto University, Department of Mechanical Engineering, P.O. Box 14400, Espoo, Finland*
E-Mail: teemu.koitto@aalto.fi

Government-enforced regulations have led to increasing demands for energy efficient solutions in the industry. To diminish the losses of hydraulic systems and to increase their energy efficiency, several pump control methods have been developed. In this work, a new experimental direct drive actuator solution, powered directly by a servo motor controlled hydraulic pump-motor, is evaluated. As an additional innovative feature, a load compensating hydraulic circuit has been introduced in order to reduce power consumption even further. The study presents results of performance measurements of this new concept.

Keywords: direct driven hydraulics, electro-hydraulic actuator, displacement-controlled hydraulics, load compensation, industrial, experimental
Target audience: industrial applications, electro-hydraulic actuators

1 Introduction

Rapid rise of government-enforced regulations leads to increasing demands for energy efficient systems in every sector of industry and society. Traditionally, many hydraulically operated stationary industrial applications have been based on valve control principle, which in actual fact means controlling the system by controlling the system's losses. To diminish the losses and to increase the system's energy efficiency, several pump control methods have been developed. One typical variant of such system is a constant pressure circuit, which is based on a constant speed variable displacement pump equipped with a pressure controller. In this case, the pump strives to maintain a constant pressure level at its outlet port regardless of the required flow rate. In some cases, where the level of required flow rate varies significantly and is, however, on average on some intermediate level, this leads to oversizing the pump in relation to the average flow need just for ensuring the maximum required flow rate. In these cases, it is reasonable to use a smaller pump together with pressure accumulator, which acts as an energy reserve and a parallel flow source whenever high flow rates are required. Besides this, the accumulator also stabilizes the source pressure.

This kind of system, with its valve-controlled actuator, is able to produce high output powers with very low response times, mainly determined by the valve's response time. However, from the point of view of energy efficiency it suffers from the need to throttle the flow that goes to the actuator, which is due to the difference between the pump maintained pressure and the actual pressure need of the actuator. Especially in mass lowering and velocity decelerating cases in general the throttling need is typically very high and causes significant power losses.

A solution for overcoming these throttling problems is valve-less closed-circuit pump control where the flow rate to the actuator is directly controlled either by controlling the rotational velocity, the displacement of the pump or both. In these solutions the flow rate of the pump and the system's pressure level are always matched to the need of the actuator and the power loss generated in the system is minimized. These pump-controlled systems have been common in mobile hydraulics for a long time, but in stationary applications interest in them has in greater extent only awakened during the last decade. The main problems hindering their wide use in these applications have been the longer response times of the controlled quantity and the higher implementation costs compared to the valve-controlled systems. The development of electric drives and the decline of their prices has, however, enabled implementing pump-controlled systems that are competitive with valve-controlled systems in these respects. This has resulted in systems that combine high energy efficiency, high dynamics and relatively low prices.

During the last decade several studies have been published comparing closed circuit pump-controlled systems with valve-controlled systems, and in some studies also with pure electro-mechanical drives /1, 2, 3/. In these studies, the properties of the speed-controlled or in addition displacement-controlled pump-control systems were found to be fully competitive or even superior in comparison in terms of dynamics and energy efficiency. Most of the studies have been mainly theoretical studies, e.g. /4, 5/, but also some applied studies have been published, e.g. /6, 7/, albeit the number of these has been low in the recent past. In addition to the above-mentioned benefits of pump-controlled closed-circuit systems, several studies also demonstrate that the noise level and warming of the system is lower than with the other system types. Since the temperature raise is low and mostly due to the long fluid transferring lines, large fluid volume isn't required for cooling purposes, a solution for further reducing of the losses is packing the drive motor – pump – actuator to a compact actuator-specific entity, which means transition from central hydraulics to decentralized hydraulics.

With pump-controlled system the high variations in required actuator power do not cause any significant changes in the system's efficiency providing that the components are sized correctly. Furthermore, by equipping the actuator with a load compensating device, the energy consumption of the system can be further reduced.

Most of the problematics concerning pump-controlled systems are related to the stability of the actuator velocity when an asymmetric (differential) cylinder is used as an actuator, or when the work cycle of the actuator includes plenty of transitions between several operation points. The latter may lead to drastically reduced energy efficiency if the pump's speed-displacement-controller is optimized for merely static operation. These problems are addressed with different controllers and control strategies /8, 9, 10/, or with an asymmetric pump, whose inlet and outlet flows are matched to the piston areas of the actuator /11/.

2 Methods

In this section, an industrial case is introduced as an example application for a novel method to achieve a more energy efficient stationary industrial application. Chapter 2.1 presents the studied industrial case implemented with traditional valve-controlled system and also the proposed novel electro-hydraulic actuator, which is realized with a direct driven hydraulic (DDH) approach and a load compensating hydraulic circuit.

2.1 Studied industrial case

The studied case is an industrial application where an actuator is required to shift a large mass continuously between two vertical positions. The distance between the positions is 260 mm and each of the movements, either lifting or lowering, should be achieved in less than one second. 700 kg mass was used during the experiments.

In this paper two different hydraulic circuits for realizing the required function are investigated and their characteristics and performance compared. At this stage of research no requirements for cooling have been considered in either of the systems.

2.1.1 Traditional valve controlled system

Currently the industrial application is operated using a traditional valve controlled system illustrated in Figure 1.

A proportional 4-way valve controls the movement of the cylinder whose position is fed back to the electronics controlling the opening of the valve, no other feedback is used in this case. Instead of a simple supply pressure control with a fixed displacement pump and a pressure relief valve the system is for energy saving purposes realized with a pressure accumulator and a pressure controlled variable displacement pump.

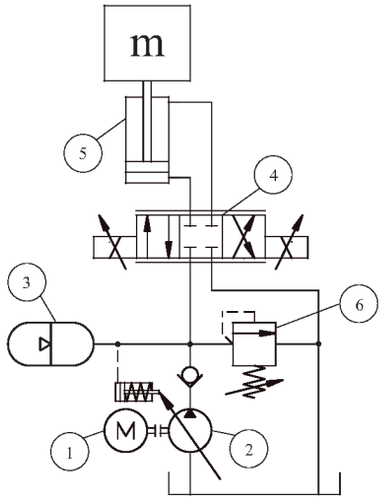

Figure 1: Traditional valve controlled implementation of studied industrial application, open circuit.

The flow needed to move the cylinder is taken from the accumulator and the displacement of the pump turns to a positive value whenever the accumulator requires a fill-up, otherwise the pump stays at zero displacement. The major components of the simulated system with their relevant data are listed in Table 1.

Number	Type	Description
1	Motor	1500 r/min
2	Pump	28 cm^3/rev
3	Accumulator	2.4 l, preload pressure 26 bar
4	Proportional valve	85 l/min, 5 bar/control edge
5	Differential cylinder	50/36 mm
6	Pressure relief valve	Opening pressure 150 bar

Table 1: Fluid power components of the simulated traditional system.

2.1.2 Electro-hydraulic actuator test setup

The second studied system is an electro-hydraulic actuator, Figure 2, where the cylinder position is controlled solely by pump rotation speed and direction. Design process for this circuit and further details on the industrial case is described in reference /12/. Pump and valves are mounted to a manifold that is directly attached to the main cylinder. Detailed component descriptions are listed in Table 2.

In the load compensating circuit, the pre-charge pressure of the 10 l accumulator (13) is converted into a vertical force, opposing the gravitational force of the load (m), with the differential cylinder. The pre-charge pressure is varied between the experiments in order to establish the circuit's energy saving potential. Three different magnitudes of load compensation were tested; a) Full in which the gravitational force of the load mass was fully compensated with opposing force of the compensator cylinder, b) Half in which half of the force of the load mass was compensated, and c) None in which the pressure in the compensating circuit was zero.

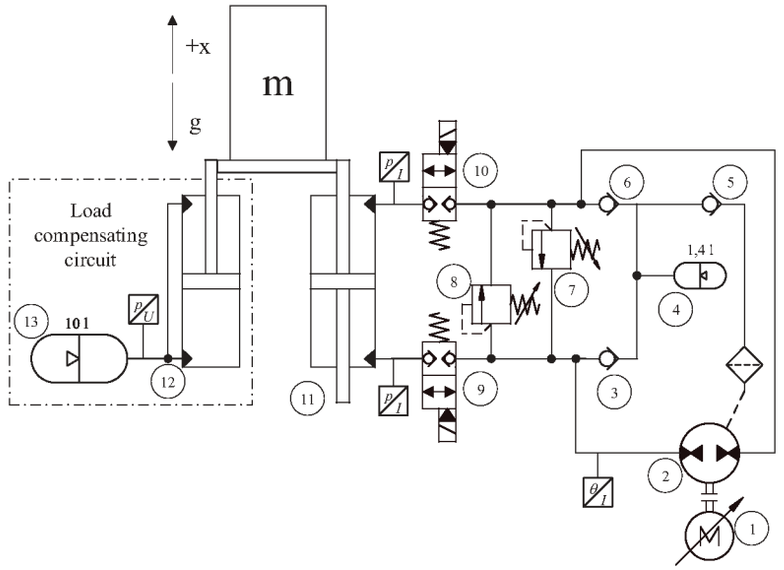

Figure 2: Novel pump controlled DDH implementation of studied industrial application, closed circuit.

Internal leakage of the pump-motor is fed back to the low-pressure side of the circuit via a filter and check valves. This section of the system also contains a small volume pressure accumulator which acts as a buffer and keeps the closed circuit filled with fluid in case of small external leaks.

Control and instrumentation of the test setup is done with a PLC as depicted in Figure 3. The PLC is running a central Sytronix controller /13, Fig. 6–12/, which is basically a PD controller, commanding the electric drive's (IndraDrive) control system that has a cascaded PI controller /14, Fig. 7–3/. Measured data from the system is acquired and the solenoids of safety valves (9, 10) are controlled through IndraControl S20 modules.

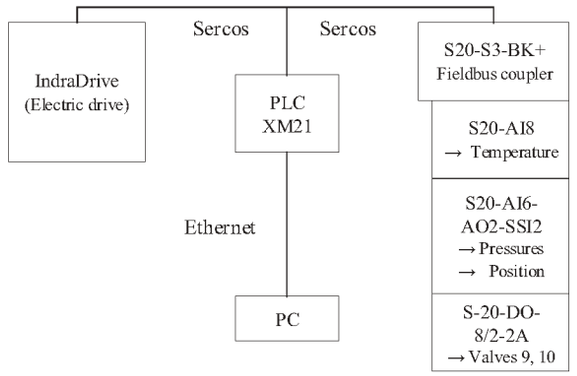

Figure 3: Control and instrumentation of the test setup.

Sytronix loop is operating with 4 ms cycle time, electric drive's velocity loop is running at 125 µs and current loop at 62.5 µs cycle time.

2.2 Simulations

The purpose of the traditional valve controlled system (Figure 1) was to be a benchmark for the novel pump controlled DDH system (Figure 2). Since measurements of an actual traditional system were not possible, the system was only simulated. Specifications for components used in the simulated system are presented in Table 1.

Performance of the simulated traditional system in terms of work cycle, cylinder transition and rise time was tuned to match the performance of the novel system in order to be able to compare the system's energy consumption characteristics in similar operational conditions. The results of the Matlab/Simulink/Simscape simulations are presented in Chapter 3.

2.3 Experiments

The experiments were made with a full scale test rig. The hydraulic circuits of the test rig are presented in Figure 2 and the components of the circuits are listed in Table 2.

	MAIN CIRCUIT		
Number	Type	Description	Details
1	Motor	Permanent magnet synchronous motor	Bosch MSK101E-0300-NN
2	Pump	Inline axial piston pump, 45 cm^3/rev	Bosch A10VZG045EZ400
11	Main cylinder	Symmetrical cylinder 50 mm piston 36 mm piston rod 300 mm stroke length	Bosch CGM1F3/50/36/300A20 /F11CKUTS42580
4	Accumulator	1,4 l bladder accumulator @ 2 bar	Bosch HAD1,4-250-1X
3,5,6	Check valve	Cracking pressure 0,3 bar	Sun hydraulics CXEE-XAN
7,8	Pressure relief valve	Opening pressure 160 bar	Bosch DBDS 10 K1X/200
9,10	Load holding valve		Bosch VEI8A2T12
	LOAD COMPENSATING CIRCUIT		
12	Cylinder	Differential cylinder 50 mm piston 36 mm piston rod 300 mm stroke length	Bosch CDM1MP5/50/36/300A20 /B11CFUMWW
13	Accumulator	10 l bladder accumulator	Bosch HAB10-330-6X

Table 2: Fluid power components of the test rig.

In addition to the fluid power components, the test rig has a significant number of electric and electronic components used for power supply and for measurement instrumentation, Table 3.

Sensors		
Pressure transducer	4-20 mA	Bosch HM 20-2X/250-C-K35
Pressure transducer	0-10 V	Bosch HM18-1X/210-V-S
Temperature sensor	4-20 mA	Ifm TA2405
Position sensor	Magnetostrictive, Analog output	Santest GYSE-A-650-N-CN-CD10
Electronics		
Motor	Permanent magnet synchronous motor	Bosch MSK101E-0300-NN
IndraDrive power section	Continuous current 95 A, Maximum current 150 A	Bosch HCS03.1E-W0150
Servo drive	Firmware version: MPB-20VRS	Bosch CSB02.1B-ET
PLC	Firmware version: MLC14VRS	Bosch XM21
Data acquisition		
I/O system	IndraControl S20	Bosch S20-S3-BK+

Table 3: Electric and electronic components of the test rig.

The motion sequence used in this study comprised a rapid lift followed by 1.5 s standstill before the load was returned to its starting positon for another standstill period, after which the next cycle began. The sequence consisted of five cycles and the same sequence was used regardless of the magnitude of load compensation (full, half, or none) used in the test. The starting position of the motion was 20 mm and the end position was 280 mm corresponding to a stroke of 260 mm. Since the maximum stroke of the cylinder was 300 mm, the actual motion left 20 mm piston travel unused in both ends. Figure 4 presents part of a motion sequence recorded with full load compensation. The position command from the PC to the Sytronix controller was of a rectangular shape (Master command), but the controller forwarded the command to the electric drive in a trapezoidal shape (Actual command). The (proprietary) controller is performing either setpoint rate limiting or motion profile planning. Throughout the study, a target velocity of 700 mm/s was specified for the actuator together with 8000 mm/s^2 acceleration in the control software.

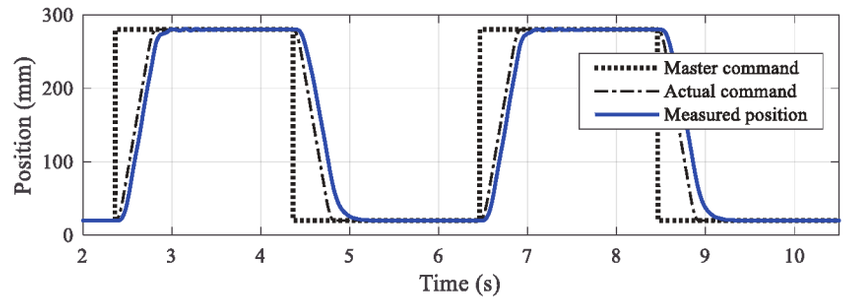

Figure 4: Part of the five cycle motion sequence.

Three test cases were run with the motion sequence, utilizing three different magnitudes of load compensation as described in Chapter 2.1.2.

The power consumption of the test setup was monitored in several locations (cf. Figures 2 and 5) in the system as the power was transferred from electric motor input power to mechanical shaft output power and onward to

hydraulic power utilized by the cylinder actuator, and finally to mechanical power delivered by the actuator to the load carriage.

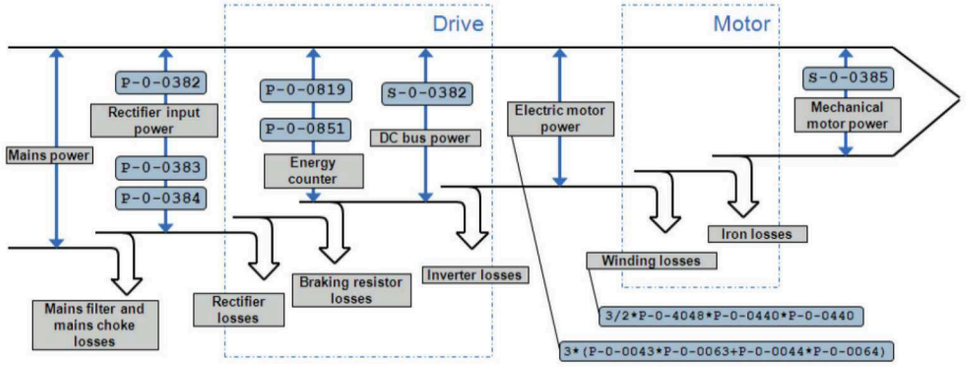

Figure 5: Energy and power parameters of the IndraDrive electric drive system. /14/

The energy counter of IndraDrive was selected to be monitored representing the energy consumption of the drive system. Electric motor power (effective electric power) transferred from the drive to the servomotor (motor input power) was calculated according to Equation (1) /14, Fig. 11–65/.

$$P_{e,m} = 3 \times (I_q U_q + I_d U_d) \quad (1)$$

Mechanical output power of the servo motor was directly recorded by one of the axis parameters (S-0-0385) of the IndraDrive system.

The hydraulic power of the pump was computed using the port pressure of the pump and the actuator's flow rate, Equation (2)

$$P_{h,p} = p_p q_{V,p} = p_p v_a A_a \quad (2)$$

Hydraulic power of the cylinder was computed using the actuator's flow rates and port pressures, Equation (3). Actuator leakage was assumed to be zero, thus the inlet and outlet flow rates are equal.

$$P_{h,a} = p_{a,in} q_{V,a} - p_{a,out} q_{V,a} = (p_{a,in} - p_{a,out}) v_a A_a \quad (3)$$

The mechanical power delivered by the actuator was computed as a product of the cylinder output force times the linear speed of the load carriage, Equation (4).

$$P_{m,a} = F_{m,a} v_a \quad (4)$$

The actuator output force was calculated as the sum of the compensated load (gravitational force minus force produced by the load compensation cylinder) and the force needed to overcome the inertia. The energy inputs and outputs of the different power transformers in the system were calculated by integrating the calculated powers.

3 Results

Simulation results of the valve controlled traditional system and the measurement results of the pump controlled DDH system are presented below. The legends used in the figures are as follows:

Master command	= Original position command	PressureA	= Pressure in lower cylinder chamber
Actual command	= Controller modified command	PressureB	= Pressure in upper cylinder chamber
Measured position	= Position of cylinder, measured	Pelec	= Electric power of electric motor
Simulated position	= Position of cylinder, simulated	Pmotor	= Mechanical power of electric motor
Lin velocity	= Linear velocity of cylinder	Ppump	= Hydraulic power of pump
Rot speed	= Rotational speed of electric motor	Pactuator	= Mechanical power of cylinder

Curves for one lifting-lowering cycle are presented; Figures 6–8 present results for the traditional valve controlled system and Figures 9–11 for the pump controlled DDH system.

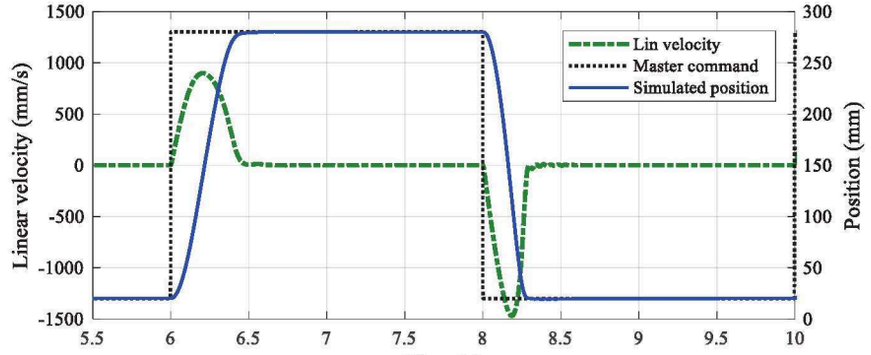

Figure 6: Simulation results; Traditional valve controlled system. Example curves for one lifting-lowering cycle, showing position reference and actual value, as well as measured linear actuation velocity.

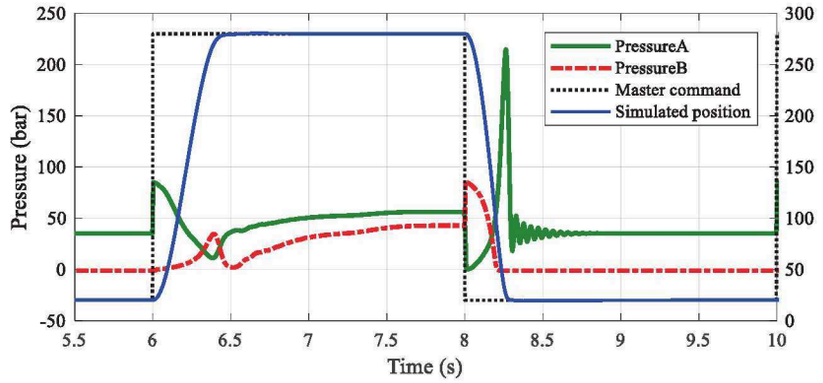

Figure 7: Simulation results; Traditional valve controlled system. Example of recorded chamber pressures together with the position curves for reference.

In Figure 8, at the beginning of the lifting phase the actuator is fed with the sum of pump and accumulator powers, and at the beginning of lowering phase in addition with the mass power, therefore during the transition phases there's a period when the actuator power is greater than the system's electric input power.

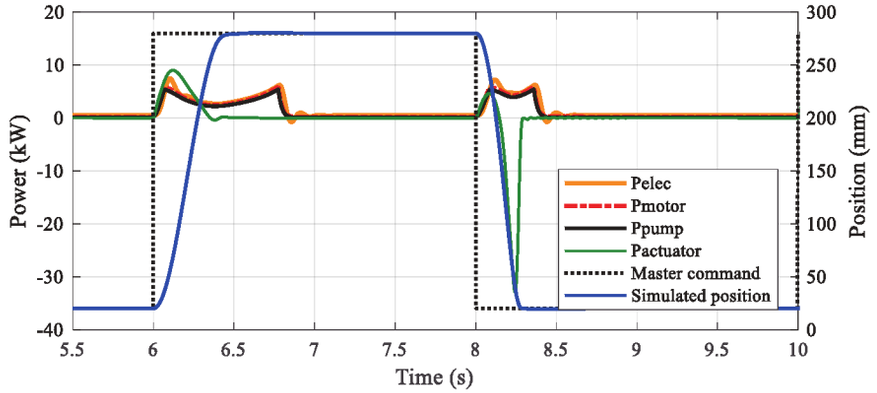

Figure 8: Simulation results; Traditional valve controlled system. Power curves corresponding to one lifting lowering cycle together with the position curves for reference.

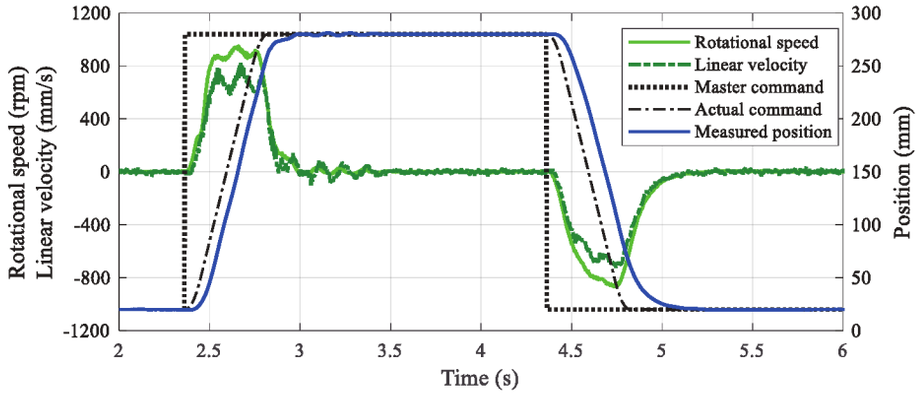

Figure 9: Experimental results; Pump controlled DDH-system. Example of one lifting-lowering cycle, showin rotational speed of motor and measured linear actuation speed as well as position reference and actual valu (test run without load compensation).

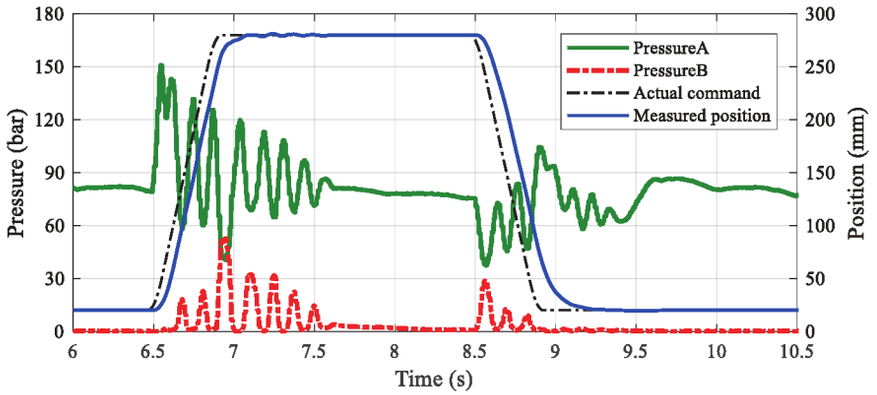

Figure 10: Experimental results; Pump controlled DDH-system. Example of chamber pressures for one lifting lowering cycle together with the position curves for reference (test without load compensation).

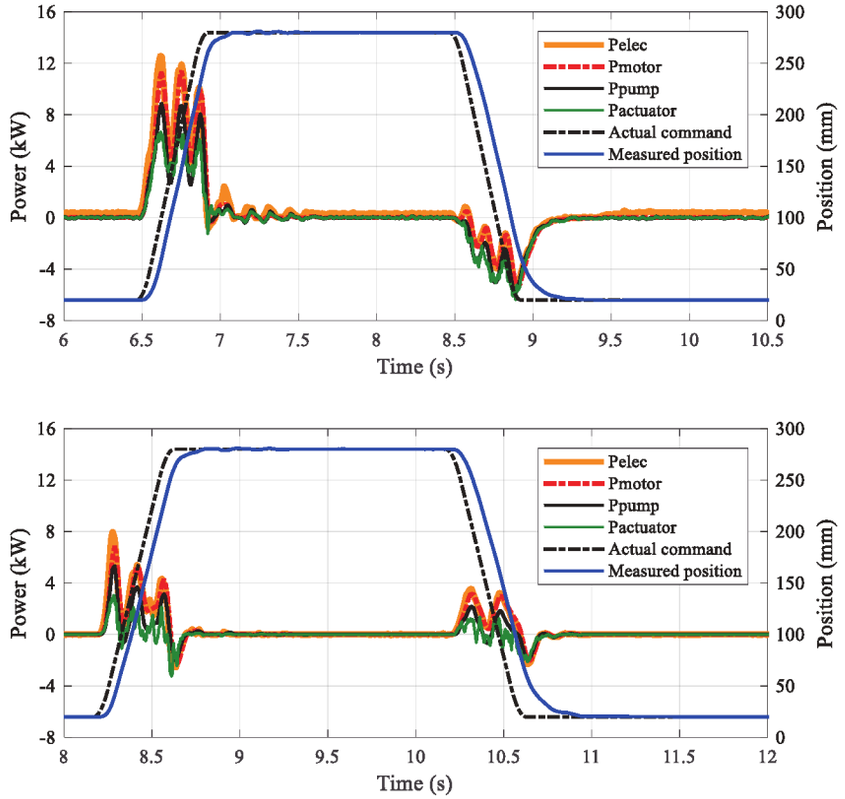

Figure 11: Experimental results; Pump controlled DDH-system. Power curves for one lifting-lowering cycle and position curves for reference. Above: test without load compensation, below: test with full load compensation.

The average energy consumption and possible recovery is shown in Table 4 as averages computed for five lifting-lowering cycles. In addition to the values per lifting-lowering cycle, separate values for lifting and lowering phases are shown for the hydraulic and mechanical energy of the actuator.

Load comp.	Energy counter $E_{e,c,c}$ [kJ]	Electric motor $E_{e,m,c}$ [kJ]	Electric motor $E_{m,m,c}$ [kJ]	Pump $E_{h,p,c}$ [kJ]	Actuator $E_{h,a,c}$ [kJ]	Actuator (lifting) $E_{h,a,lift}$ [kJ]	Actuator (lowering) $E_{h,a,lower}$ [kJ]	Actuator (lifting) $E_{m,a,lift}$ [kJ]	Actuator (lowering) $E_{m,a,lower}$ [kJ]
Full	1.80	1.67	1.59	0.75	0.75	0.99	0.42	0.15	0.10*
Half	2.27	2.03	1.69	0.73	0.73	1.65	0.20	0.99	0.93*
None	3.83	3.24	1.79	0.59	0.59	2.34	0.12	1.75	1.74*
Trad.sys.	N/A	6.37	5.13	4.45	3.03	2.11	0.91	2.63**	

N/A : Value is not available from simulation * : Recovery ** : Combined value for lifting and lowering

Table 4: Average energy inputs/outputs. During lowering phase, mechanical energy is recovered by actuator.

During the lifting phase the actuators of both systems require a certain hydraulic input energy to overcome the loading of the mass and friction forces. This energy is presented as parameter $E_{h,a,lift}$ in Table 4. During the lowering phase the mass's potential energy acts as the actuator's driving force which together with the hydraulic driving force generated by the pressure in the motoring (upper) chamber of the actuator pushes the piston downwards thus generating mechanical power (Figures 8, 11). This power is transmitted to the pumping (lower) chamber of the actuator via the piston and transformed into hydraulic power/energy, which can be recovered. The variable $E_{h,a,lower}$ expresses the hydraulic input energy that is required in the upper chamber to drive the actuator to the lower position from its upper position. The recoverable energy generated during the lowering phase is presented in Table 5. In the traditional system, energy is not recovered, but converted into heat in the system's control valve.

Load comp.	Energy counter $E_{e,c,rec}$ [kJ]	Electric motor $E_{e,m,rec}$ [kJ]	Electric motor $E_{m,m,rec}$ [kJ]	Pump $E_{h,p,rec}$ [kJ]	Actuator $E_{h,a,rec}$ [kJ]	Actuator $E_{m,a,rec}$ [kJ]
Full	-0.56*	-0.54*	-0.51*	-0.15*	-0.15*	0.10
Half	0.26	0.28	0.31	0.66	0.66	0.93
None	1.09	1.13	1.18	1.55	1.55	1.74
Trad.sys.	N/A	N/A	N/A	N/A	N/A	N/A

N/A : Energy recovery not available in simulated system * : energy is not recoverable

Table 5: Average energy inputs/outputs during the lowering phase in the different test runs.

4 Discussion

In this research, a typical working cycle of a stationary industrial lifting application was studied. The energy inputs and outputs of the main components in both a traditional fluid power implementation (Figure 1), and a novel pump controlled implementation (Figure 2) were compared. The traditional valve controlled implementation was modelled and simulated with Matlab/Simulink/Simscape for reference purposes against the pump controlled DDH implementation. The model was tuned to match the measurement results of the DDH system to enable straight comparison between these two systems. Although actual dimensioned component data was used in the models available in Simscape, the somewhat simplified formulation of these models may affect the simulation results. In practice, the losses of the simulated system, characterized by the difference in energy consumptions between the electric input energy of the drive motor and the mechanical output energy of the cylinder actuator (Table 4), may be somewhat underestimated because of the simplifications.

The DDH implementation was studied experimentally. In all three test cases (with different load compensation), the actuator tracked the position reference of the Sytronics controller reasonably well. There were only small oscillations after the target position had been reached, Figures 10–11. Also, the target stroke time set for this study (260 mm in less than one second), was reached. For example the rise time for reaching 98 % of the stroke for the different load compensation cases were: no compensation 0.55 s, half 0.53 s, and full compensation 0.54 s.

The results manifest strong pressure fluctuations (Figure 10) during both lifting and lowering phases. These were concluded to arise because of the mechanical imperfections in the test rig, which had excessive clearances between the vertical guide rails and the rollers of the load carriage. During its motion, the carriage hit both the sides and bottom of the rails several times in an oscillatory way and thus the rollers were not carrying the carriage throughout the movement like they were expected to. This caused changing friction forces, which in turn caused some variation in the actuator's load. Because the relation between cylinder velocity and the rotational speed of the pump depends on the cylinder load, e.g. /11/, both the cylinder's velocity and pump's rotational speed varied during the movement which was observed in the measurements (e.g., Figure 9). The phase shift between these variations caused pulsation in the inflow of the actuator's working chamber. This in turn resulted in high pulsation in the working chamber's pressure because of the relatively low chamber volume and the low compressibility of the fluid. The pulsation continued for a while after the actuator had reached its target position, this was concluded to result from the spring-mass nature of the system and also from the fact that the pump also kept on pulsating at very low speeds until the actuator settled to its target position causing similar inflow pulsation of the working chamber as during the fast movement. The measured pressure pulsations are naturally reflected in the calculated powers of Figure 11. In order to reach smoother operation, the rail-roller system should be modified.

The results show that the energy consumption of the DDH system is considerably lower than that of the traditional valve-controlled system. This is perhaps best reflected in the $E_{e,m,c}$ values (electric energy input to the motor) in Table 4. The differences in energy consumptions were due to two major factors; firstly, the hydraulic losses of DDH system were lower because of the absence of the actuator controlling valve, and secondly, because the closed circuit DDH was able to recover energy, which was not possible in the simulated open circuit valve-controlled system. Furthermore, the utilization of load compensation reduced energy consumption quite significantly. If using a DDH system without load compensation reduced the electric energy input by 49 % (3.24 kJ vs. 6.37 kJ), applying full load compensation further reduced the electric energy consumption by 48 % (1.67 kJ vs. 3.24 kJ). Thus the combined effect of using a DDH system with load compensation resulted in a reduction of 74 %.

The ability of DDH to recover energy due to regenerative braking depends on the level of load compensation (Table 5). Without load compensation the quantity of recovered energy is higher than with lower compensation levels, but also the consumption of energy is simultaneously higher. Actually, with full load compensation there is no energy to be recovered. This can also be deduced by comparing the power curves in Figure 11.

Load compensation decreases the load and pressure in the main circuit, which enables the use of a smaller diameter hydraulic cylinder. This can be used to increase actuator velocity or to decrease pump size, of which the latter is extremely valuable as it would decrease the rotational inertia of the pump enhancing its dynamics and make the system cost-wise more competitive compared to a traditional valve-controlled system.

5 Conclusion

This research has shown that pump controlled fluid power significantly reduces energy consumption in an industrial application for rapid-stroke handling of high loads, compared to a simulated valve controlled system based on traditional fluid power components. The energy consumption of the pump controlled DDH system was measured in experiments in a full scale test rig equipped with a hydraulic load compensation circuit and utilizing a motion sequence of five consecutive lifting-lowering actions. By using the DDH system, it was found that the electric energy input could be reduced by 49 % compared to the simulated traditional system. Moreover, a reduction of 74 % could be achieved when full hydraulic load compensation was used together with the DDH system. Indeed, utilizing a load compensation circuit appears to be an economical and simple solution for bringing down energy costs in this type of application. In summary, energy consumption values of the DDH system were in all tests substantially lower than the energy consumption values of the traditional system, indicating a large potential for energy savings in industrial fluid power systems.

The presented findings were based on short test runs. Therefore further studies should involve investigating the long term characteristics of the DDH system including, e.g., how the thermal conditions evolve during continuous usage and the possible need for cooling.

6 Acknowledgements

This research was enabled by the financial support of Tekes (the Finnish Funding Agency for Innovation, project EL-Zon), and internal funding from the Department of Mechanical Engineering at Aalto University, Finland.

The contributions of D.Sc. (Tech) Henri Hänninen, M.Sc. (Tech) Antti Sinkkonen, Mr. Ville Vidqvist, and Mr. Rainio Kuisma in making the test rig operational are greatly appreciated.

Nomenclature

Variable	*Description*	*Unit*
A_a	Piston area of actuator	[m^2]
$E_{e,c,c}$	Electric energy input value of energy counter for one lifting-lowering cycle	[kJ]
$E_{e,c,rec}$	Electric energy recoverable from frequency converter during the lowering phase	[kJ]
$E_{e,m,c}$	Electric energy input to electric motor for one lifting-lowering cycle	[kJ]
$E_{e,m,rec}$	Electric energy recoverable from servo motor during the lowering phase	[kJ]
$E_{h,a,c}$	Hydraulic energy input of actuator for one lifting-lowering cycle	[kJ]
$E_{h,a,lift}$	Hydraulic energy input of actuator for one lifting phase	[kJ]
$E_{h,a,lower}$	Hydraulic energy input of actuator for one lowering phase	[kJ]
$E_{h,a,rec}$	Hydraulic energy recoverable from actuator during the lowering phase	[kJ]
$E_{h,p,c}$	Hydraulic energy output of pump for one lifting-lowering cycle	[kJ]
$E_{h,p,rec}$	Hydraulic energy recoverable from pump during the lowering phase	[kJ]
$E_{m,a,lift}$	Mechanical energy output of actuator for one lift phase	[kJ]
$E_{m,a,lower}$	Mechanical energy recovered by actuator during one lowering phase (= $E_{m,a,rec}$)	[kJ]
$E_{m,m,c}$	Mechanical energy output from electric motor for one lifting-lowering cycle	[kJ]
$E_{m,m,rec}$	Mechanical energy recoverable from servo motor shaft during the lowering phase	[kJ]
$F_{m,a}$	Actuator force	[N]
I_d	Flux generating current	[A]
I_q	Torque generating current	[A]
$p_{a,in}$	Pressure in the working chamber of actuator	[Pa]
$p_{a,out}$	Pressure in the counter acting chamber of actuator	[Pa]
p_p	Pressure at pump outlet port	[Pa]
$P_{e,m}$	Electric input power of servo motor	[W]
$P_{h,a}$	Hydraulic input power of actuator	[W]
$P_{h,p}$	Hydraulic power of pump	[W]
$P_{m,a}$	Mechanical output power of actuator	[W]
$q_{v,a}$	Inlet and outlet flow rates of actuator	[m^3/s]
$q_{v,p}$	Pump outlet flow rate	[m^3/s]
U_d	Flux generating voltage	[V]
U_q	Torque generating voltage	[V]
v_a	Actuator velocity	[m/s]

References

/1/ Michel, S., Weber, J., *Energy-efficient electrohydraulic compact drives for low power applications*, Fluid Power and Motion Control FPMC 2012, September 12–14, 2012, Bath, Great Britain. ISBN 978-0-86197-187-9.

/2/ Boes, C., Helbig, A., *Electro hydrostatic actuators for industrial applications*, 9th International Fluid Power Conference, 9. IFK, March 24–26, 2014, Aachen, Germany. ISBN 978-3-9816480-1-0.

/3/ Helbig, A., Boes, C., *Electric hydrostatic actuation - modular building blocks for industrial applications*, 10th International Fluid Power Conference, 10. IFK, March 8–10, 2016, Dresden, Germany.

/4/ Räcklebe, S., Helduser, S., *Electric hydrostatic drive – a concept for the clamping unit of a high-speed 245 injection moulding machine*, Power Transmission and Motion Control PTMC 2007, September 12–14, 2007, Bath, Great Britain. ISBN 978-0-86197-140-4.

/5/ Tašner, T., Les, K., Tič, V., Lovrec, D., *Energy efficiency of different electrohydraulic drives*, 9th International Fluid Power Conference, 9. IFK, March 24–26, 2014, Aachen, Germany. ISBN 978-3-9816480-2-7.

/6/ Müller, K., Dorn, U., *Variable Speed Drives - Customer Benefits in Injection Molding Machines and Presses*, 7th International Fluid Power Conference, 7. IFK, March 22–24, 2010, Aachen, Germany.

/7/ Brahmer, B., *CLDP – Hybrid drive using servo pump in closed loop*, 8th International Fluid Power Conference, 8. IFK, March 26–28, 2012, Dresden, Germany.

/8/ Willkomm, J., Wahler, M., Weber, J., *Model Predictive Control of Speed-Variable Variable-Displacement Pumps to Optimize Energy Efficiency*, 9th International Fluid Power Conference, 9. IFK, March 24–26, 2014, Aachen, Germany. ISBN 978-3-9816480-0-3.

/9/ Willkomm, J., Wahler, M., Weber, J., *Potentials of Speed and Displacement Variable Pumps in Hydraulic Applications*, 10th International Fluid Power Conference, 10. IFK, March 8–10, 2016, Dresden, Germany.

/10/ Sun, Y., Imam, A., Wu, C., Sepehri, N., *Stability study of a pump-controlled circuit for single rod cylinders via the concept of Lyapunov exponents*, ASME/BATH 2017 Symposium on Fluid Power and Motion Control FPMC 2017, October 16–19, 2017, Sarasota, Florida, USA. ISBN 978-0-86197-187-9.

/11/ Quan, L., Ge, L., Wang, B. C., Li, B., Zhao, B., Lu, Z., *Performance of speed variable asymmetric pump controlled asymmetric hydraulic cylinder*, The 10th JFPS International Symposium on Fluid Power 2017, October 24–27, 2017, Fukuoka, Japan.

/12/ Hänninen, H., Minav T., Pietola M., *Replacing a constant pressure valve controlled system with a pump controlled system*, Proc. BATH/AASME 2016 Symposium on Fluid Power and Motion Control FPMC 2016, September 7-9, 2016, Bath, UK.

/13/ Rexroth HydraulicDrive 13VRS Central Controller Functional Description, Edition 2, R911336586, Bosch Rexroth AG, Germany, 2013

/14/ *IndraDrive MPx-20 Functions,* Application Manual, Edition 1, R911345608, Bosch Rexroth AG, Germany, 2017.